Collapse Probability Assessment of a 4-Story RC Frame under Post-Earthquake Fire Scenario

Moradi, M.[1], Tavakoli, H.R.[2][*] and Abdollahzade, GH.R.[3]

[1] Ph.D. Candidate, Department of Civil Engineering, Babol Noshirvani University of Technology, Babol, Iran.
[2] Associate Professor, Department of Civil Engineering, Babol Noshirvani University of Technology, Babol, Iran.
[3] Professor, Department of Civil Engineering, Babol Noshirvani University of Technology, Babol, Iran.

ABSTRACT: Post-earthquake fire is a rare event with catastrophic consequences. The occurrence of fire after an earthquake can cause a catastrophe. Structural damage during earthquake loading affects the capacity of the element in the fire following earthquake loading. In this study, the probability of collapse and collapse time probability of a 4 story RC frame under earthquake and post-earthquake fire loading are assessed. At first structural sections are modeled in ABAQUS and heat transfer analysis is performed in them. After the results extraction of heat transfer analysis, the frame is modeled in openSees software base on the Finite Element method. For assessment seismic collapse probability, Incremental Dynamic Analysis (IDA) is conducted and the fragility curve is extracted for three performance levels. Then, seismic and fire loading are applied to frame consecutively and collapse probability is calculated. The probability distribution functions and the cumulative distribution function of the structural collapse time are calculated in the post-earthquake fire analysis. The results show that increasing PGA increases collapse probability and decrease collapse time in the RC frame under post-earthquake fire loading.

Keywords: Collapse Time, Heat Transfer, Post-Earthquake Fire, Probability Assessment, RC Frame.

1. Introduction

Lateral loading has various effects on the structure. Blast and earthquake loading may damage the structural elements (Tavakoli a Kiakojouri, 2015). Each load creates a different response in structures. Some responses are tangible, while most responses are subtle. An earthquake may cause secondary consequences In addition to the structural damaged (Tavakoli and Afrapoli, 2018).

Earthquake reduces the strength of structures against further loads (Moradi and Abdolmohammadi, 2020). In addition to the damages which are caused by the earthquake itself, it has some subsequent consequences. These consequences in

[*] Corresponding author E-mail: tavakoli@nit.ac.ir

nature are landslide and tsunami. Moreover, earthquake itself cause some dangers for structures (Moradi et al., 2019). Fire and Post-Earthquake Fire (PEF) are considered to be a serious threat to human societies. This is a rare event with a lot of probable consequences (Moradi et al., 2021). PEF is a real threat in high-density places. This kind of fire has been known as a destructive and severe force in the last century (Albuquerque et al., 2018). Different structural elements lose their strength and stability on exposure to high temperatures. This reduction in strength will increase if the elements are damaged by seismic loads (Elhami Khorasani and Garlock, 2017). Elhami Khorasani (2015) examined the behavior of steel frames under PEF loading probabilistically and deterministically. PEF is a great hazard for the place with a high population density (Ronagh and Behnam, 2012). Structural safety decreases rapidly against natural disasters such as PEF. Many structures such as RC buildings have been damaged by PEF events. The stiffness and capacity of structural members reduce when exposed to extreme heat.

The evaluation of the response of structures under multi-hazard scenarios has been developed in recent years. The damage to gas pipes during an earthquake and gas leak can set the structure on fire after the earthquake. The occurrence of an internal or external explosion may be accompanied by fire. What matters first of all is the safety of the structure for fire prevention and, then, fire resistance of the structure (Behnam et al., 2016). The Post-earthquake fire is known as a destructive force in the last century (Wen et al., 2016). In recent years, the research approaches have increased in the field of multi-hazards events such as PEF. Jelinek et al. (2017) studied the resistance of steel buildings under post-earthquake fire scenarios. Khorasani et al. (2017) studied data-driven probabilistic post-earthquake fire ignition model for a community. Chicchi and Varma (2018) reviewed post-earthquake fire assessment of steel buildings in the United States.

Hutchinson et al. (2018) studied physical damage evolution during earthquake and post-earthquake fire testing of a mid-rise cold-formed steel framed building. Vitorino et al. (2020) studied evaluation of post-earthquake fire capacity of reinforced concrete elements. Tang et al. (2020) studied post-earthquake strength assessment of a steel bridge considering material strength degradation. During Nigatta Earthquake in 2004, the earthquake caused directly 9 fire events (Elhami Khorasani, 2015).

Despite the notable number of studies investigating post-earthquake fire scenarios, the effect of damage caused by earthquake on the structural performance of buildings under the fire loading scenario has not been sufficiently investigated. Such damage may cause notable differences in the behavior damaged reinforced concrete buildings due to the occurrence of cracking and spalling.

In this study, a 4-story RC frame is considered as a structure subjected to post-earthquake fire loading. After seismic loading, the fragility curve is provided and the probability of exceeding performance levels is calculated. Then seismic and fire loads applied to frame and collapse times in post-earthquake fire are extracted. Finally, the fragility curve for post-earthquake loading at Intensity Measures (IM) is provided.

2. Methodology

2.1. Probability

Probability of structural collapse can be calculated from the following equation (Abdollahzadeh and Faghihmaleki, 2018):

$$P[Coll]_{EQ} = P[Coll|EQ] \times P[EQ] \qquad (1)$$

where P[$Coll$]$_{EQ}$: is the annual probability of collapse limit state of the building when the structure is exposed to an earthquake. P[$Coll$/EQ]: is the seismic fragility curve and P[EQ]: is the annual rate of seismic activities in the structural site.

If fire to be considered as a calamitous event in a building, the annual probability of structural collapse under fire loading can be deduced from Eq. (2):

$$P[Collapse]_{Fire} = P[Collapse|Fire] \times P[Fire] \quad (2)$$

where P[$Collapse$]$_{Fire}$: is the annual probability of collapse limit state of the building when the structure is exposed to a fire loading. P[$Collapse/Fire$]: is the fire fragility curve and P[$Fire$]: is the annual rate of the fire event.

If a PEF to be considered as an event under the following condition, then:

$$P[PEF] = P[Fire|Earthquake] \quad (3)$$
$$P[Earthquake|Fire] = 0 \quad (4)$$

The annual probability of structural collapse under PEF loading can be deduced from Eq. (5).

$$P[Collapse]_{PEF} = P[Collapse|PEF] \times P[PEF] \quad (5)$$

Substitution Eq. (3) into Eq. (5) results:

$$P[Collapse]_{PEF} = P[Collapse|PEF] \times P[Fire|Earthquake] \quad (6)$$

On the other hand:

$$P[Fire|Earthqkae] = P[Fire \cap Earthquake] \times P[Earthqkae] \quad (7)$$

Substitution Eq. (6) into Eq. (7) results:

$$P[Collapse]_{PEF} = P[Collapse|PEF] \times P[Fire \cap Earthquake] \times P[Earthqkae] \quad (8)$$

Story drift, maximum records acceleration, the stories that fire has been accrued in that story and fire load are the parameters that are considered as engineering parameters. The drift of stories in each PGA under PEF and earthquake have been calculated and then the probability of exceed of structure from limit state have been calculated.

2.2. Seismic Load

Intact and damaged structures have different responses to fire loading. Earthquakes could cause damage to structures. Damaged and the response of the structure to seismic loads can be expressed as three performance levels base on FEMA 356 (BSSC, 2000). Immediate Occupancy (IO), Life Safety (LS) and Collapse Prevention (CP) are these three performance levels. Structural performance levels can be expressed as maximum story drifts. Based on FEMA 356 (2000), the maximum story drifts equal to 1% under seismic loads represents the IO performance level and cause minor crack and damage in RC sections (Behnama and Ronagh, 2013). The maximum story drifts equal to 2% represent LS performance level and cause major crack and damage in RC sections. In this study, the effect of cracking and spalling caused by a seismic load on heat transfer analysis in reinforced concrete sections is considered (based on Wen et al. (2016) and Behnam and Ronagh (2013)). The effect of the cracks in the heat transfer analysis has been applied in the areas of the plastic hinges (FEMA 356, 2000). These cracks have been created due to the seismic load and its effect has only been observed in the boundary conditions of the heat transfer analysis (Mohammadizade and Jafarzade, 2021).

In this study, incremental dynamic analysis is used to perform seismic load to the RC frame. After each step of the dynamic analysis, the maximum drift of frame is extracted and the performance level of RC frame is evaluated. Based on the performance levels, cracking is applied to sections for each seismic load. Ten ground motion records were selected for applying IDA analysis. Table 1 shows the selected ground motion records characteristics. Each record was scaled from 0.1g to 1g and was applied to frame.

Table 1. Characteristics of ground motion records

Event	Year	Station	Mag.	Vs (m/s)	PGA (g)
Niigata	2004	NIGH11	6.63	375	0.59
Kobe	1995	Nishi-Akashi	6.9	609	0.48
Loma Prieta	1989	Corralitos	6.93	462	0.645
Northridge	1994	LA Dam	6.69	628	0.426
San Fernado	1971	Lake Hughes #12	6.61	602	0.38
Bam	2003	Bam	6.6	487	0.807
Hector Mine	1999	Hector	7.13	726	0.265
Kocaeli	1999	Arcelik	7.51	523	0.21
Landers	1992	Yermo Fire St.	7.28	353	0.15
Manjil	1990	Abhar	7.37	302	0.13

2.3. Heat Transfer Analysis

Concrete sections (presented in Table 2) were modeled in ABAQUS and thermal properties assigned them. Based on the structural performance presented in Section 3-1-1, minor and major crack were assigned to the concrete section and heat transfer analysis was performed according to fire load (presented in Figure 1). Heat transfer analysis of sections depends on a variety of factors. Density, heat transfer coefficient and specific heat capacity are the most important parameters of heat transfer in various materials. Due to the fire load, the heat flow transfers from the outermost part of the section were exposed to the heat towards the cooler areas further away from the fire.

In this study, the parameters of thermal conductivity and specific heat capacity are considered as a function of temperature. In Figure 2, the values of thermal conductivity and specific heat capacity of concrete materials are shown. The density of concrete materials is equal to 2.4 g/cm^3. Standard fire load had been used in most researches as fire loading.
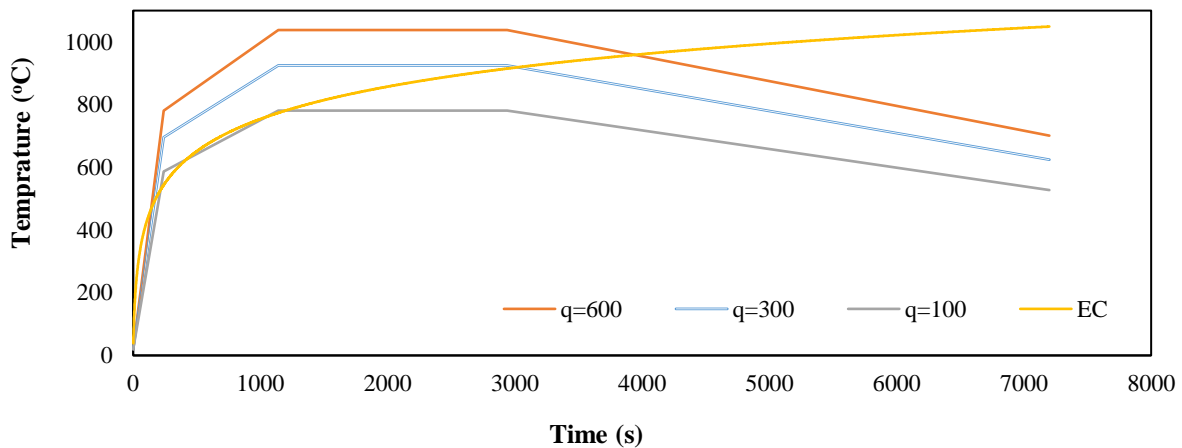
Fig. 1. Time-temperature curves of the study
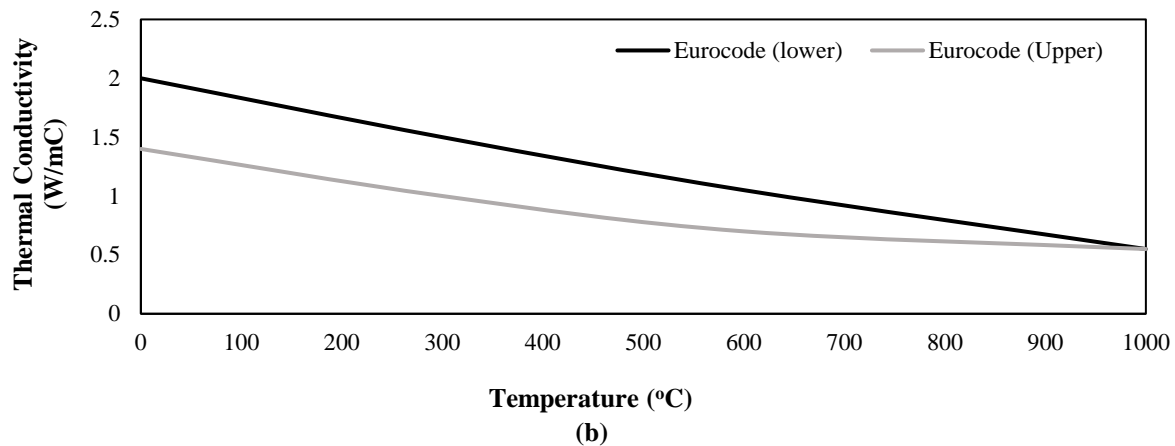

(a)
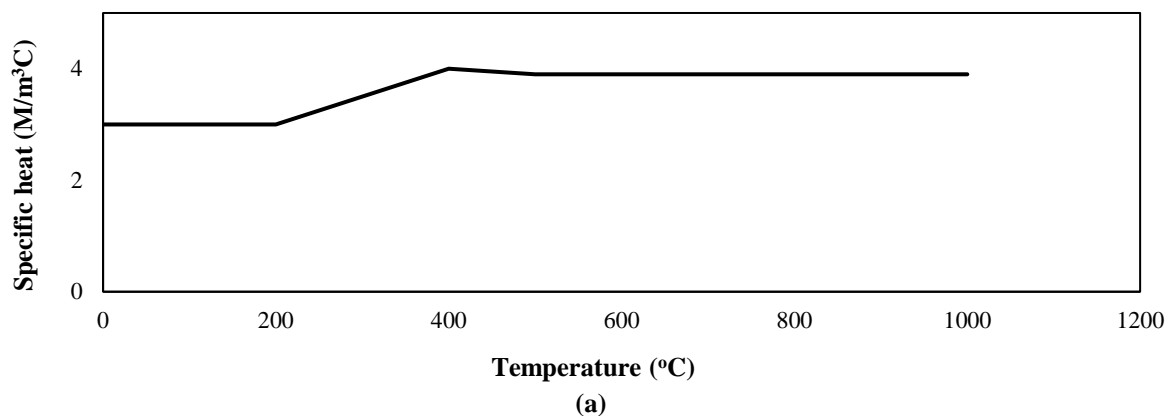
Fig. 2. Changes in the thermal properties of the concrete materials versus an increase in temperature: a) Specific heat capacity; and b) Thermal conductivity coefficient (Moradi et al., 2020)

Although Opensees performs heat transfer analysis, for greater accuracy, ABAQUS software is used to heat transfer analysis. Heat transfer analysis in the reinforced concrete section is the only elementary part of this research. For the thermal modeling of the reinforced concrete sections, the following characteristics have been used:

Special heat and thermal conductivity is shown in Figure 3. The density of concrete materials is equal to 2.4 g/cm^3. RC section was analysis by film coefficient 25 W/m^{2}C and emissivity 0.7. All of these parameters were extracted from EN 1992-1-2 (2004).

According to Wen (2016) and Behnam and Ronagh (2013) studies, cracking and spalling cause a faster transfer of temperature to reinforcements. Therefore, it is necessary to consider cracking and spalling due to seismic loading effect in modeling the post-earthquake fire. In this research, based on the Wen and Behnam's studies, the spalling effect (caused by the seismic load) is only intended to accelerate heat transfer. In fact, with the transfer of boundary conditions from the cover to the reinforcement, the effect of spalling is considered. Therefore, the effect of spalling due to fire has not been considered in this study.

In this study, the effect of cracking and spalling caused by a seismic load on heat transfer in reinforced concrete sections is considered (based on Wen et al. (2016) and Behnam and Ronagh (2013)). Spalling makes it possible to separate a piece of concrete from the reinforced concrete section. This allows the boundary conditions to move from the cover to the center of the cross section.

For example, if a member is at the damage level of 4, the thermal load is placed in the boundary conditions of the reinforcements. This causes the temperature in the reinforcement concrete section to be higher than the normal RC section.

The temperature-time curves are extracted for different fire loads (presented in Figure 1) at various concrete section's heights. Figure 3 and 4 show an example of heat transfer in concrete sections with minor and major cracks for the EC fire load. In this figure, *H*: is the distance from the half of cross-section and *d*: is the total height of the section. When the thermal analysis is conducted for different concrete sections, the temperature-time curves are extracted and used for the analysis by OpenSees software.

2.4. PEF Scenario

In the second step of the analysis, a 4-story RC frame is modeled in OpenSees. Then the seismic and thermal load is applied to it consecutively. After seismic-thermal loading, the response of frame and collapse times (if there are exist) are evaluated. For applying seismic-thermal analysis after each ground motion a time-temperature curve according to Section 3-1 applied to 4-story RC frame. Four fire loads

were applied to frame in four situations after each seismic loading.

The first situation is applying fire load to the entire fire story (F1). In the second situation, the fire load is applied to the entire first and second stories (F2). In the third and the fourth situations, fire load is applied to entire of stories 1, 2 and 3 and entire of the frame, respectively (F3 and F4). The situations and location of the fire load are shown in Figure 5. Therefore, after each seismic loading, sixteen fire loading scenarios are applied to the frame separately. Fire load is applied to frame in four types and four situations. The seismic load is applied to frame according to IDA analysis.

Each ground motion is scaled from 0.1g to 1g (in the step of 0.1g). Therefore, one hundred ground motions are applied to the RC frame. Generally, one thousand and sixty hundred PEF scenarios were considered for this study. After each PEF

loading, probability of collapse in the structure was assessed and fragility curve for PEF scenario was calculated and presented.

The fire loads were applied to the frame for two hours. Two criteria were considered for structural collapse. First, maximum drift ratio reaches 0.02 during fire loading. Second, the analysis does not converge during fire loading and structural elements loss bearing capacity and failure had been occurred (Moradi et al., 2020).

The Seismic and thermal analysis in the RC frame was applied continuously. So the residual strain effects due to the seismic loading was automatically considered in thermal loading. The time of a sudden increase in the vertical displacement of the middle span of the beam is considered as the failure criterion of the structure under PPF and PEF loads (Behnam and Ronagh, 2013).
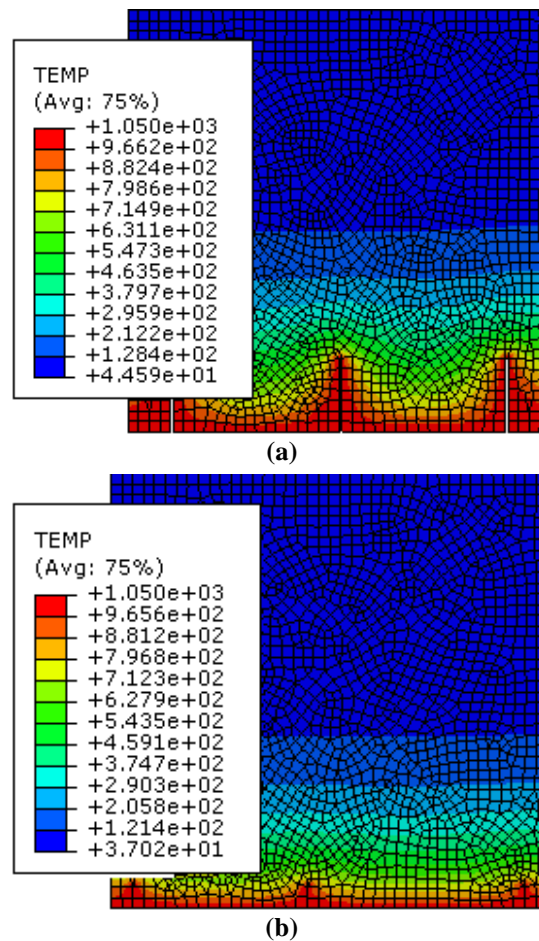

(a)

(b)

Fig. 3. Heat transfer in the concrete section under fire load proposed by EC: a) Section with major cracks; and b) Section with minor cracks
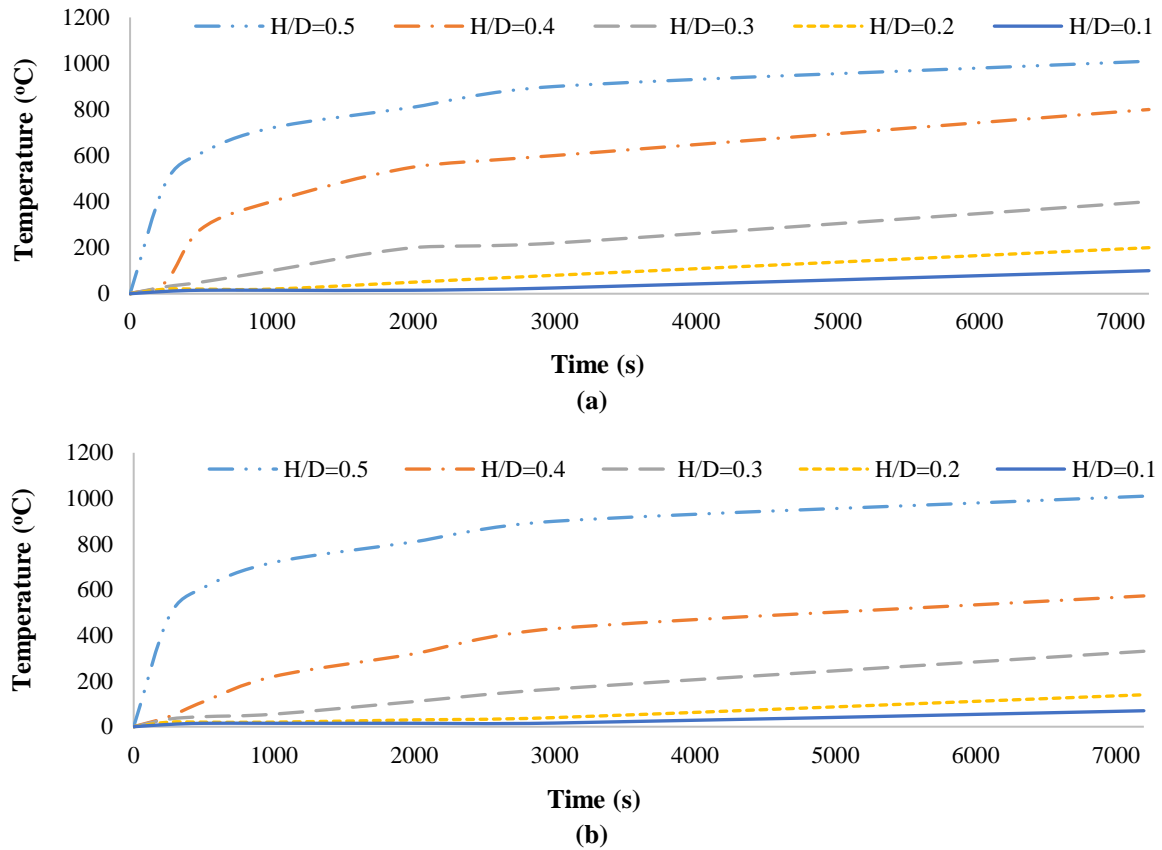
Fig. 4. Temperature-time curves for the depth of cross-section in the concrete section under fire load proposed by EC: a) Section with major cracks; and b) Section with minor cracks
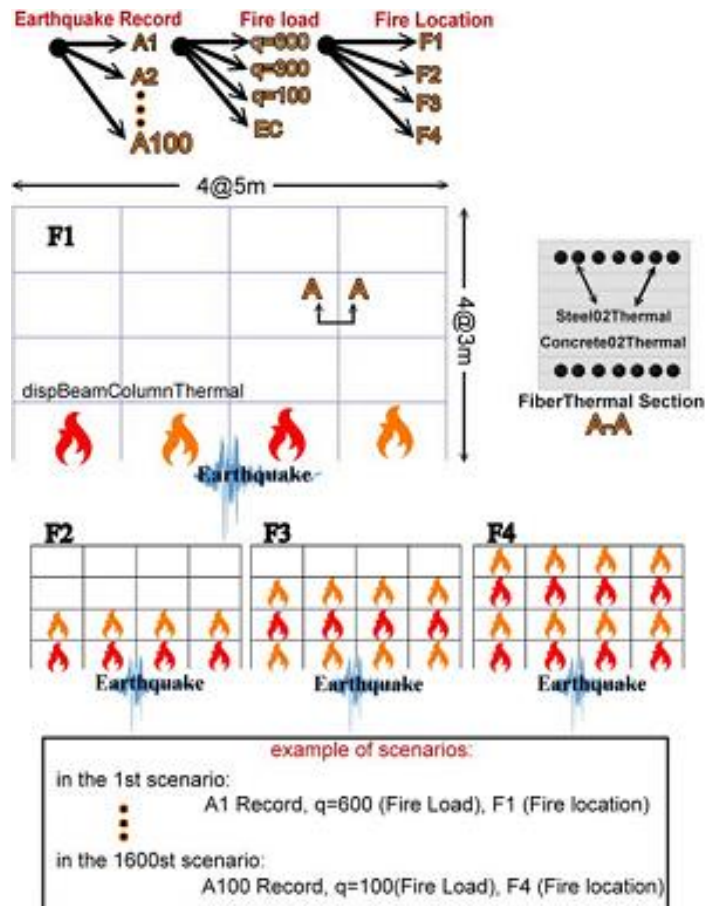

Fig. 5. Schematic figure of structural models and applied loads of the research

2.5. Numerical Modeling

A four-story RC frame is selected for seismic-thermal analysis. The selected case was loaded and designed based on ACI 318-08 (2007) Code. This structure was made using concrete with the compressive strength of 2.8e7 N/m² and reinforcement bars with the yield stress of 4.8e8 N/m². The dead and live loads were 400 kgf/m² and 200 kgf/m², respectively. It was assumed that the frame is loaded with full dead load and 25% live load during the analysis. The frame was considered for residential use, and the soil was of D type. The heights of the story were considered 3 m. It was assumed that frame is in the form of 4-span with 5 m length. Table 2 summarizes the design of the 4-story RC frame.

The nonlinear behavior of the 4-story frame under seismic loading was modeled by using rotational springs. The frame was modeled with dispBeamColumnThermal elements that were connected with zero-length elements in the OpenSees environment. Thermal modeling in OpenSees was conducted with the dispBeamColumnThermal element. Each beam or column element was divided into ten dispBeamColumnThermal elements. Three integration points were assigned to each dispBeamColumnThermal elements. The sections of the beam and column were considered as fiber sections. The time-temperature curves were assigned to the fiber for each fire load.

Concrete02thermal and Steel02thermal were used for concrete and steel material, respectively. Characteristics of Concrete02thermal and Steel02thermal are shown in Table 3. In this table $f_{sp,\theta}$: is the strength of steel proportional limit at the considered temperature, $f_{sy\theta}$: is the steel yield strength at the considered temperature, f_{yk}: is the yield strength at 20 °C, $E_{s,\theta}$: is the modulus of elasticity of steel at the considered temperature, $\varepsilon_{c\theta}$: is the concrete strain at the maximum compressive strength, and $f_{c\theta}$: is the maximum concrete compressive strength. Figure 6 shows a schematic representation of the thermal modeling of the elements.

2.6. Verification

The numerical modeling in this study was validated by the comparison between numerical modeling and experimental work by Imani et al. (2014). They exposed a ductile concrete-filled double-skin tube column to cyclic loads as load control and then applied the fire loading. Afterward, they assessed vertical displacements and durability during the thermal loading. Figure 7 graphically illustrates Imani's experimental model.

The mechanical-thermal materials of Concrete02Thermal and Steel02Thermal were employed as concrete and steel materials for the modeling of this composite column. The dispBeamColumnThermal was used for the elements with mechanical-thermal properties. The column was modeled and loaded in accordance with Imani et al. (2014). Figure 8 shows the vertical displacement-time curves for the experimental and numerical models in this study. The results of the numerical modeling study show that the vertical displacement of column falls within the range of vertical displacements in various gauges for the top of the column in the experimental model. The failure time in the numerical model of this study is accurate enough compared to Imani's experimental model. The vertical displacement in the numerical model is close to the mean value of gauges 1 and 2 in the experimental model (Figure 8), which indicates the accuracy of numerical results in this study.

Table 2. Structural sections

Story	Column		Beam		
	Dimensions	Rebar	Dimensions	Top	Bottom
1	50 × 50	20Q20	40 × 40	8Q18	6Q18
2	50 × 50	20Q18	40 × 40	6Q18	5Q18
3	40 × 40	16Q16	35 × 35	5Q16	4Q16
4	35 × 35	16Q14	35 × 35	5Q12	4Q12

Table 3. Changes of concrete and steel material parameters according to different temperatures

	Concrete02thermal		Steel02thermal		
-	$f_{c,\theta}/f_{ck}$	$\varepsilon_{c,\theta}$	$f_{sy,\theta}/f_{yk}$	$f_{sp,\theta}/f_{yk}$	$E_{s,\theta}/E_s$
20	1	0.0025	1	1	1
100	1	0.004	1	0.96	1
200	0.95	0.0055	1	0.92	0.87
300	0.85	0.007	1	0.81	0.72
400	0.75	0.01	0.94	0.63	0.56
500	0.6	0.015	0.67	0.44	0.4
600	0.45	0.025	0.4	0.26	0.24
700	0.3	0.025	0.12	0.08	0.08
800	0.15	0.025	0.11	0.06	0.06
900	0.08	0.025	0.08	0.05	0.05
1000	0.04	0.025	0.05	0.03	0.03
1100	0.01	0.025	0.03	0.02	0.02
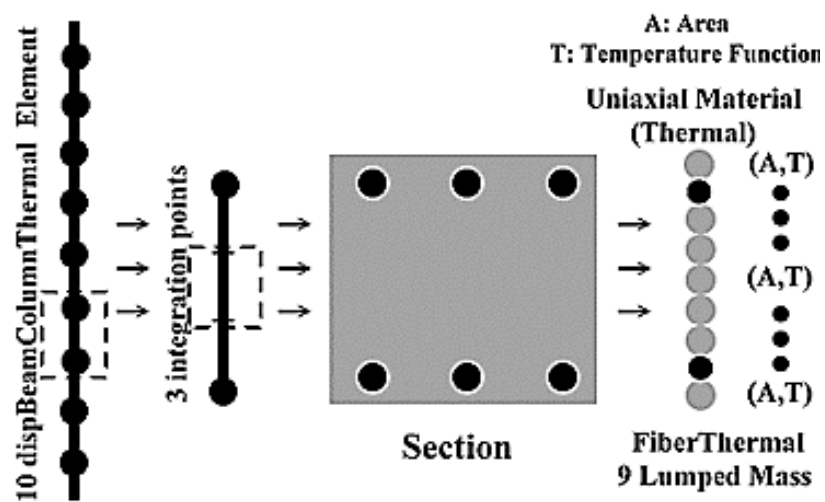
Fig. 6. Schematic figure of mechanical and thermal elements modeling in OpenSees (Moradi et al., 2020)
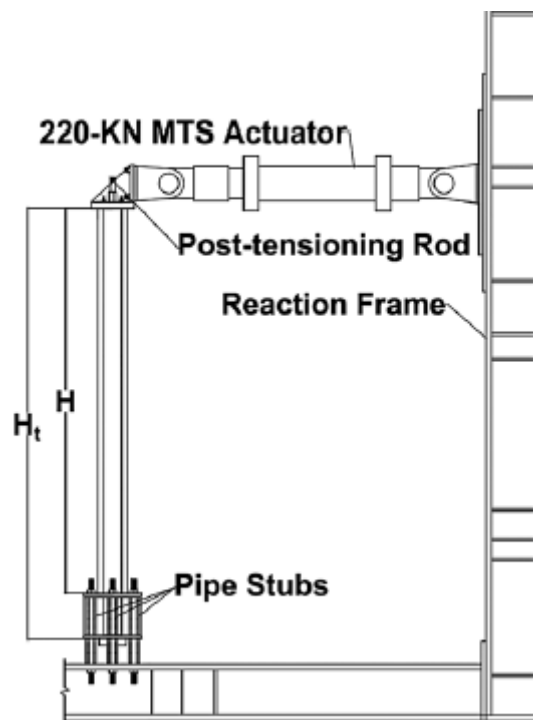
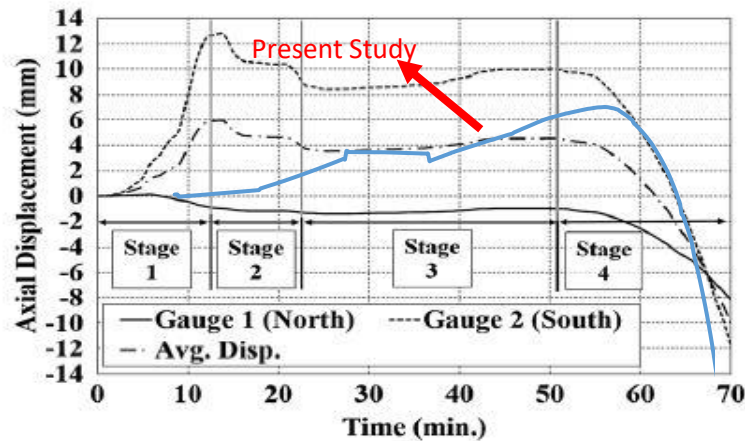**Fig. 7.** Imani's experimental model (Imani et al., 2014)

Fig. 8. Vertical displacement-time curve in Imani's experimental model and numerical analysis in this study

3. Analysis of the Results

3.1. Seismic Analysis

In the first step of the study, 4-story RC frame was subjected to seismic loading. IDA analysis was conducted using ten different ground motions scaled to different PGA (0.1g to 1g). After each analysis, the response of the frame was assessed and the maximum story drift was extracted. The probabilistic distribution of maximum frame drift is shown in Figure 9. Based on this figure, the maximum drift values of the RC frame have a quasi-normal distribution. Drift values have an average equal to 0.01401 and a standard deviation equal to 0.00901. Normal distribution for this average and the standard deviation is also shown. It is observed that thirty-four percent of all maximum drift is equal or less than the amount specified in the IO performance level. Forty-one percent of all maximum drift is between IO and LS levels. Twenty-four percent of all maximum drift

of frame under seismic loading is between LS and CP levels and one percent is at CP level. According to Section 2, P[*Collapse/EQ*] is the fragility of the frame under seismic loading. The fragility curve of the RC frame is presented in Figure 10 for three different performance levels (IO, LS, and CP).

The limit state for IO, LS and CP performance levels were considered equal to 0.01, 0.02 and 0.04 respectively, and the probability of exceedance over these performance levels was calculated based on the normal distribution function. In this study intensity measure was considered as PGA and fragility curve presented in terms of the PGA. Based on Figure 10 probability of exceedance at PGA = 1g is equal to 0.955 for the IO performance level. The corresponding values were equal to 0.74 and 0.08 for LS and CP performance levels respectively. The collapse probability of this frame was equal to 0.02 at PGA = 0.9g.
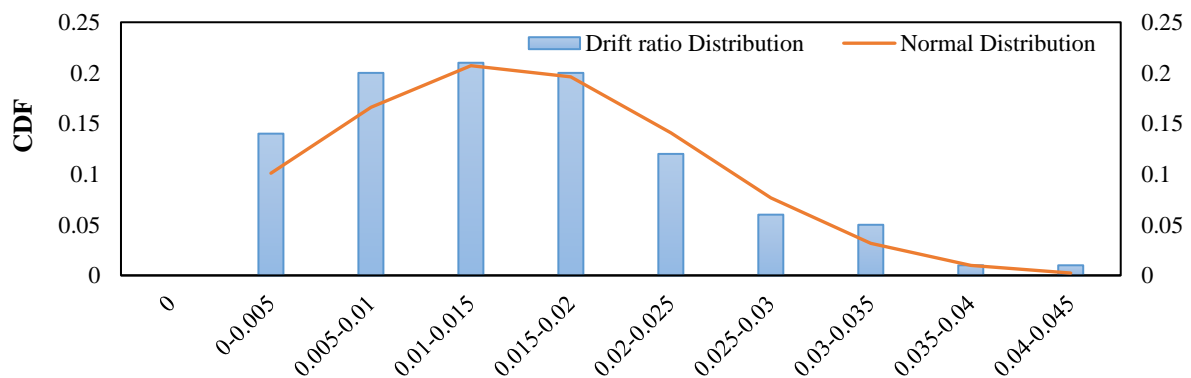

Fig. 9. Probabilistic Distribution Function (PDF) for the maximum drift of the frame in earthquake scenario
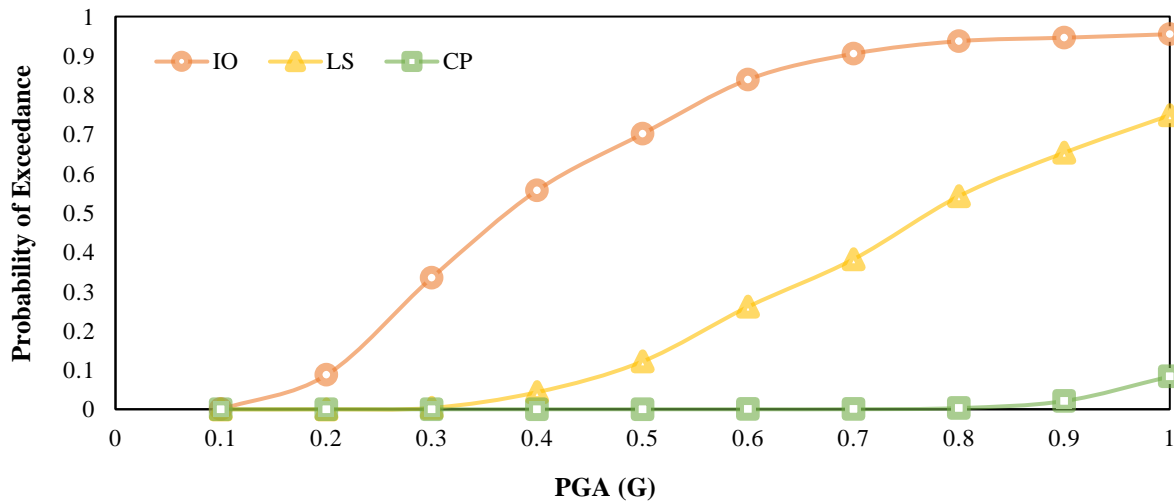
Fig. 10. Fragility curve of the structure under earthquake scenario

3.2. PEF Analysis

After seismic analysis and extraction of fragility curve (P[*Collapse*/*EQ*]), the 4-story RC frame was subjected to PEF loading. The frame response under PEF loading was assessment and the probability of collapse for this frame was calculated. Collapse time is the most important parameter in this study. It is assumed that the collapse criterion in the PEF scenario, is reaching the drift values of more than 0.02. In Figure 11, time history curve for the story drift ratio during a PEF scenario (Earthquake: Northridge, PGA = 0.8g, location: F2, Fire load = 100 MJ/m^2) is shown.

Based on Figure 11 maximum drift ratio in the earthquake scenario was equal to 0.027. Therefore, the performance of this frame under seismic loading was at LS level. In fire following earthquake loading,

drift ratio in story 1 and 2 increased. Since the drift ratio was less than 0.02, the collapse had not happened during fire loading but permanent drift increased. The result of seismic-thermal analysis showed that fire loading increased the response of the RC frame after seismic loading but may not lead to collapse. Collapse may happen with increasing fire load. In Figure 12, time history curve for the story drift ratio during a PEF scenario (Earthquake: Northridge, PGA = 0.8g, location: F2, fire load = 600 MJ/m^2) is shown. Comparison of Figures 11 and 12 shows that increasing load fire increases the response of the RC frame under fire following earthquake loading. Figure 12 indicates the drift ratio in story two was increased from 0.00128 to 0.02 after 1200 seconds during fire loading that means collapse was occurred after about 21 minutes during PEF scenario.
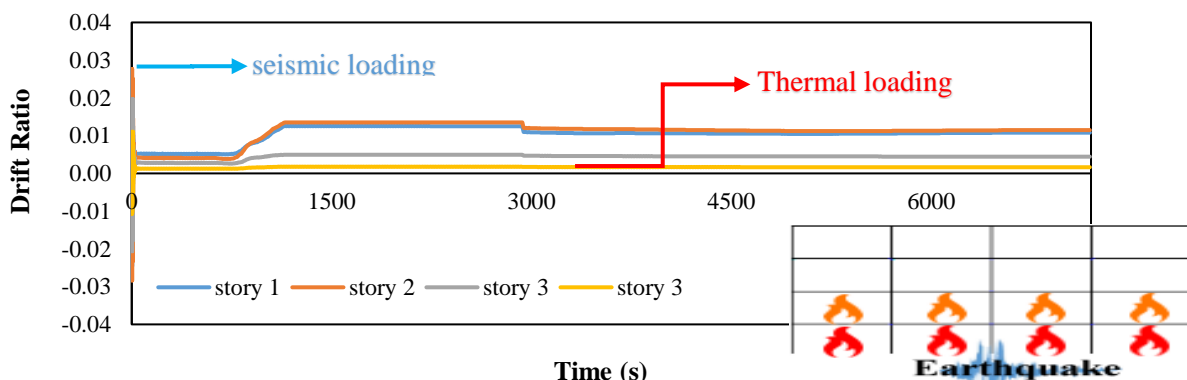

Fig. 11. The time-history curve for the drift of the considered frame in the Northridge earthquake scenario with PGA equal to 0.8g and fire load equal to 100 MJ/m^2 and F2 situation

Fig. 12. The time-history curve for the drift of the considered frame in the Northridge earthquake scenario with PGA equal to 0.8g and fire load equal to 600 MJ/m² and F2 situation
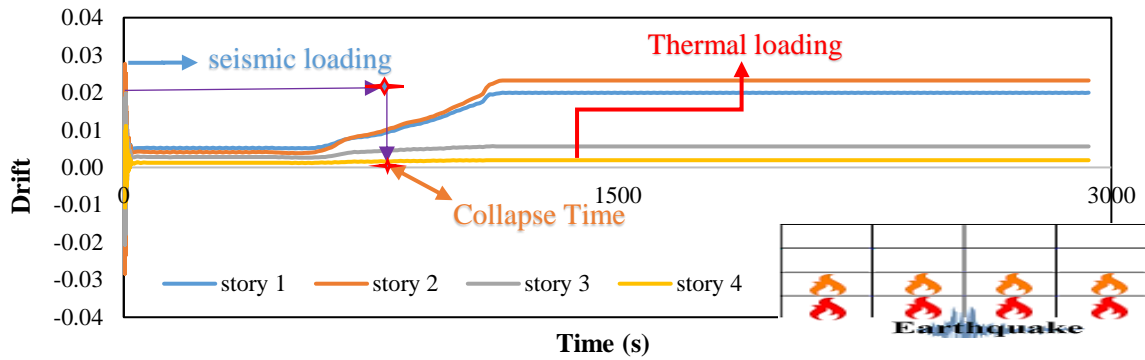
In Figure 13, time history curve of axial force for first story middle column under bam ground motion records and fire load of EC in situation F4 is shown. Based on this figure, earthquake and fire following earthquake did not lead to the collapse in PGA = 0.1g to PGA = 0.5g. In PGA equal to 0.6g fire following earthquake was lead to collapse after 5420 seconds. Indeed, considering performance level and corresponding cracking in sections decreased fire resistance time and this reduction is higher in the higher PGA.

In Figure 14 shear-moment curve for the middle beam of the first story under Loma grand motion record and EC fire load is shown. Based on this figure earthquake and fire following earthquake did not lead to collapse in PGA equal to 0.1 and 0.5g but collapse accrued in PGA equal to 1g at 2600 second after applying fire load. In the ground motions with PGA = 0.1g and 0.5g, shear and moment at first increased under fire loading and then decreased because of high temperature, bud this decrease did not lead to collapse. In the ground motions with PGA = 1g cracking, residual displacement and strength loss were lead to collapse during fire loading after 2600 seconds.
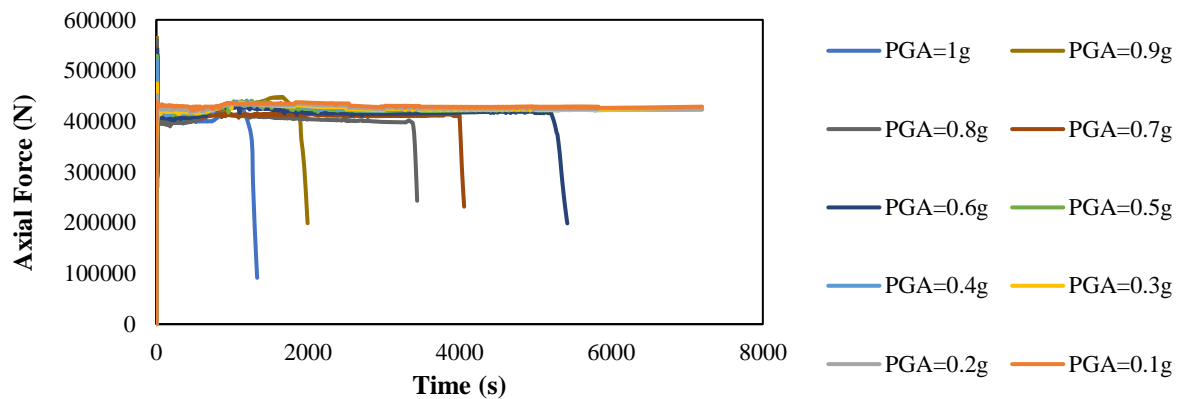

Fig. 13. The time-history curve of axial force in the middle column under PEF scenario
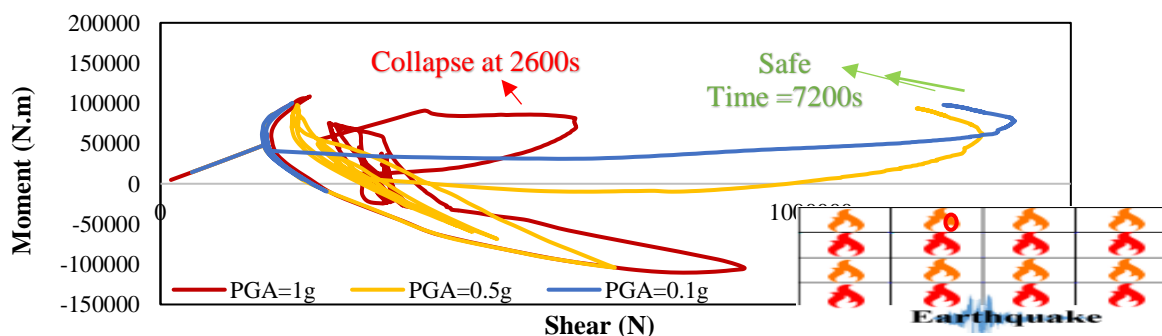

Fig. 14. Shear-Moment curve of Beam in PEF scenarios

Presented PEF scenarios in Section 3-2 were applied to RC frame and durability (collapse mode or safe mode) of the frame under PEF loading was assessed. The probabilistic distribution of the collapse time in the structure was calculated and presented in Figure 14. According to this figure in seventy percent of all PEF scenarios, the post-earthquake fire was not caused to collapse of the RC frame. The fire was lead to the collapse in thirty percent of PEF scenario (collapse time was less than 120 minutes). Probability distribution and cumulative distribution of analysis time were shown in Figures 15 and 16.

Figure 15 shows that in a probabilistic distribution, the collapse time (less than 120 minutes) does not follow a particular trend. Therefore, Bernoulli distribution has been used to assess the probability of collapse and the total number of collapse modes to the total analysis modes is considered as the probability of collapse. In order to evaluate the effect of fire's situation on the collapse time of the RC frame, the PDF and CDF curves are extracted individually for the F1,

F2, F3, and F4 situations (Figures 17 and 18). Probabilistic distribution functions and cumulative distribution probability of the collapse time indicate that in F4 fire situations, the probability of collapse is more than other models.

The results show, number of spans and stories subjected to fire loading effect on strength of RC frame in post-earthquake fire loading. Increasing fire locations increases the probability of collapse under PEF loading. The probability distribution functions show that in almost all cases, the situation F4 and F3 have more probability density at different times. Probability of collapse, in this case study, for F4 and F1 situation was equal to 0.395 and 0.192 respectively. The results of all analysis indicate that the probability of collapse (as a definite event) is equal to 0.3. This value shows 30% of all PEF scenarios were lead to collapse, however, in the earthquake scenarios, 8% of all scenarios were lead to collapse (probability of exceedance from CP performance level).
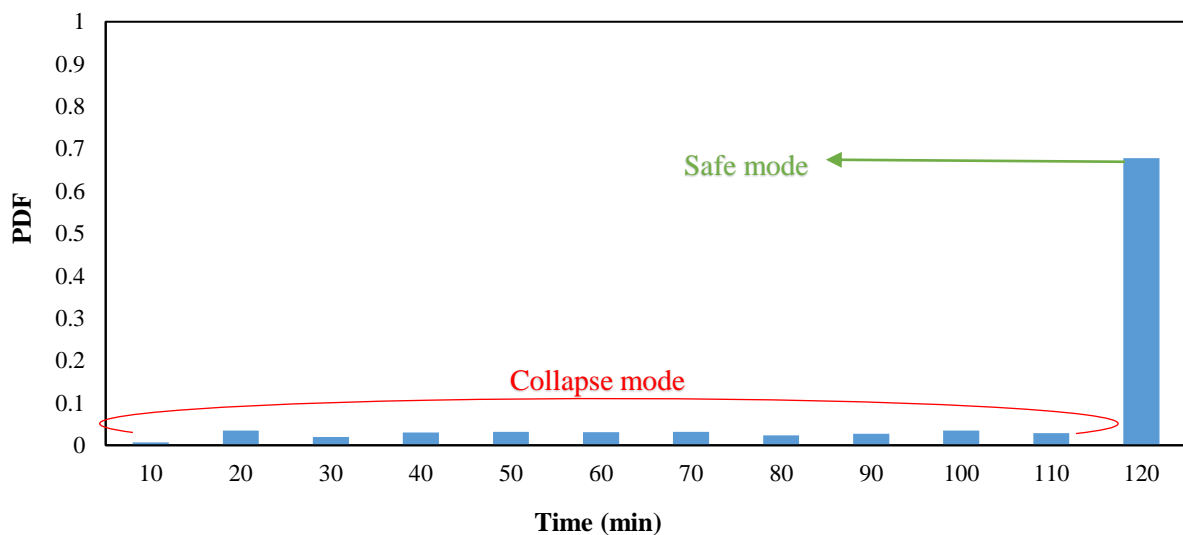

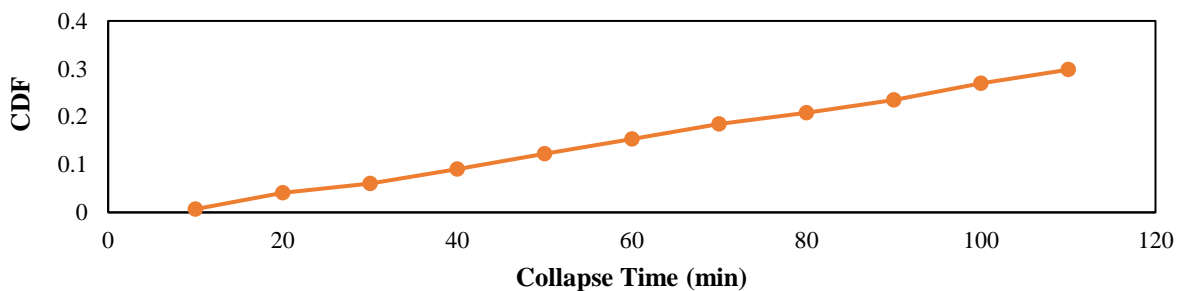**Fig. 15.** Probabilistic distribution of the collapse time

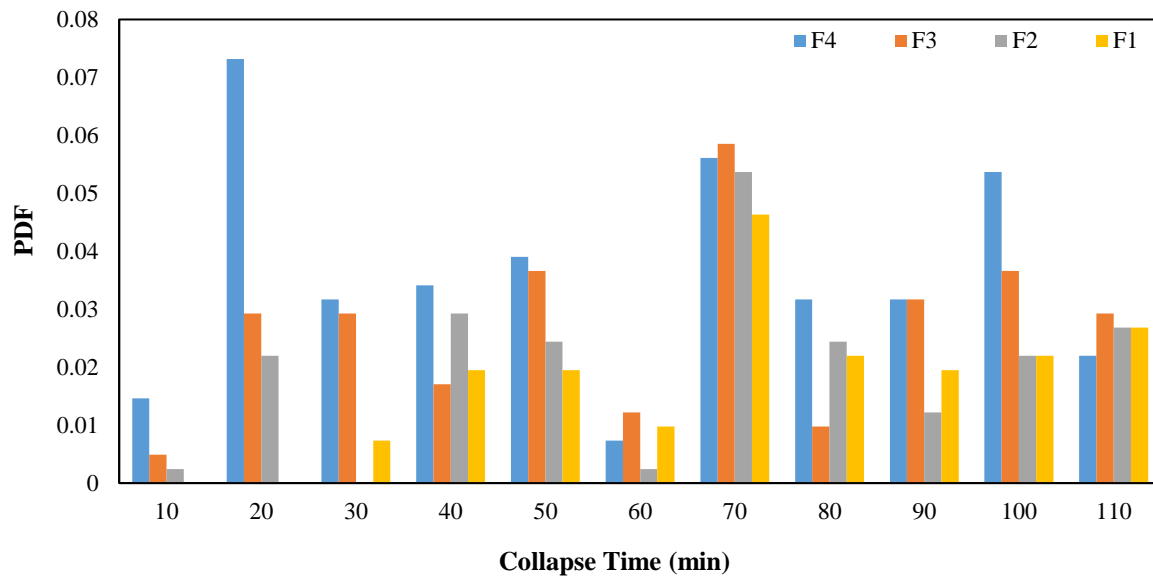**Fig. 16.** Cumulative distribution function of collapse time

Fig. 17. The probability distribution function of the collapse time in different situations
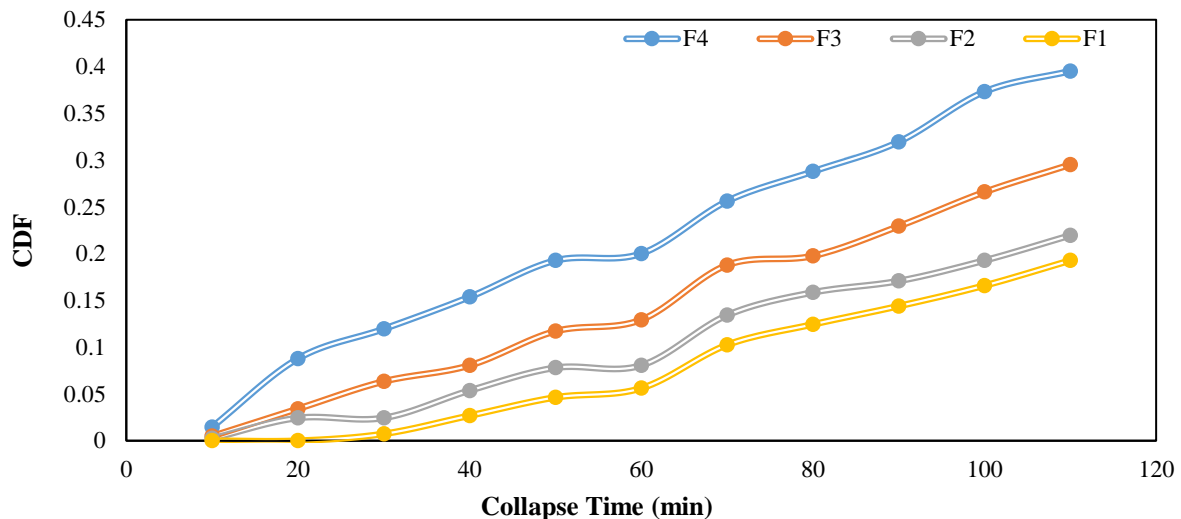

Fig. 18. Cumulative distribution of the probability of collapse time in different situations

The probability of collapse in the PEF scenario is extracted for the different PGA. Collapse probability on condition of PEF occurrence (P[$collapse/fire \cap EQ$]) will be equal to the fragility curve in different intensity measures (PGA). As stated, the probability of collapse in the PEF scenario is calculated by Bernoulli's distribution function. Figure 19 shows the collapse probability curve on the condition of PEF scenario (P[$collapse/fire \cap EQ$]) (fragility curve). Based on this figure, the probability of collapse due to a PEF is zero at a maximum acceleration of less than 0.3g. As PGA increases, the probability of collapse due to a PEF loading is increased. Based on Figure 19, 9 percent of all fire following an earthquake with PGA = 0.4g loading lead to collapse. The fragility curve of PEF loading shows the probability of collapse in the fire following an earthquake with PGA = 0.8g is equal to 0.625. This value shows in 62.5 percent of fire loading in an RC frame subjected to an earthquake whit PGA = 0.8g, the frame will collapse in less than two hours.
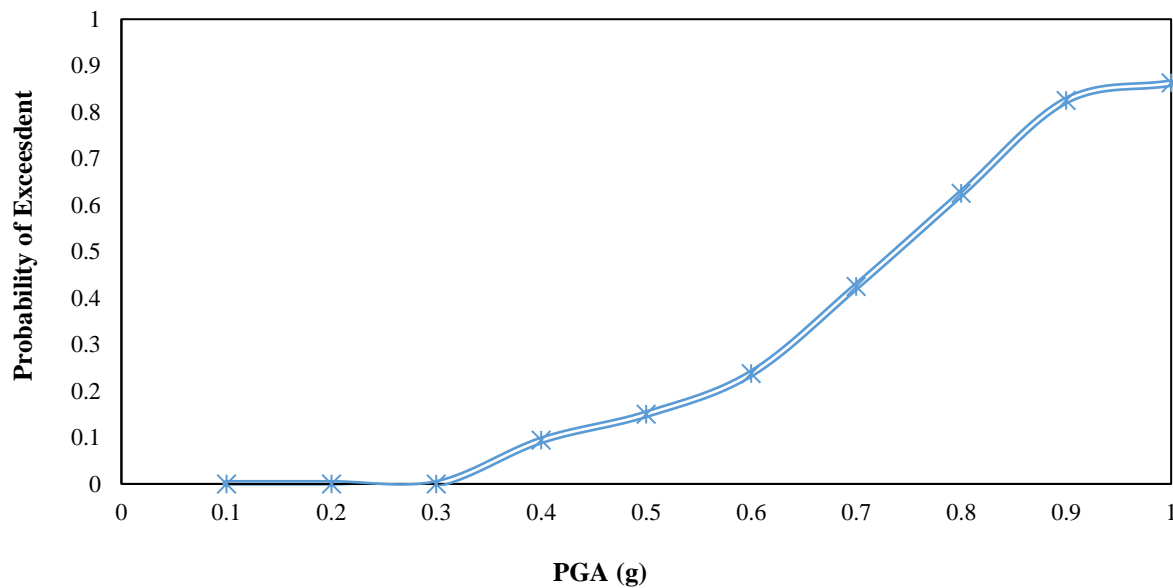
Fig. 19. Fragility curve of the reinforced concrete frame in PEF scenario

Based on Eq. (6), the probability of collapse of structures due to the PEF scenario depends on P[*collapse/fire* ∩ *EQ*], P[*fire/EQ*] and P[*EQ*]. P[*fire/EQ*] is a non-engineering parameter that relies on many factors, including structural and population density, safety factors in construction and materials of the structure. According to the researchers conducted in the reference (Khorasani et al., 2016), the possibility of the PEF (P[*fire/EQ*]) at a maximum acceleration of 1g in a region with a population density of 10,000 to 40,000 people per square kilometer, can range from about 0.15 to 0.9. This value will be fewer for the smaller maximum acceleration. In this research, assuming a population density of 15,000 km², the probability of a PEF event is 0.2. The annual rate of earthquake occurrence (P[*EQ*]) usually considered being 10% for conventional structures, during the lifespan of the building. This earthquake usually has an occurrence probability of about 0.0021 per year with a returning period of 475 years, P[*fire/EQ*] = 0.0021. So, the maximum probability of collapse because of PEF scenario (P[*collapse/fire* ∩ *EQ*]$_{max}$) happens in the maximum acceleration of 1g, which is about 0.86. Therefore, the most probability of annual collapse due to PEF in the 4-story

RC frame can be calculated as follows:

$$P[collapse]=P[collapse \mid (Fire \cap EQ)] \times P[Fire \mid EQ] \times P[EQ]$$

$$\rightarrow P[collapse]=0.86 \times 0.2 \times 0.0021$$

$$\rightarrow P[collapse] = 0.00036$$

So, the rate of collapse due to PEF in the intended frame of the research is equal to 0.00036 (0.036 percent). In the following, the probability of collapse of the structure was assessed in the only definite occurrence of earthquake scenario and the definite occurrence scenario of a PEF. Figure 20 indicates the fragility curves for different performance levels in the earthquake scenario and the probability of collapse in the PEF scenario for a 4-story RC frame. According to this figure, the probability of collapse in this research due to the PEF scenario at maximum accelerations of less than 0.7 g is very similar to the fragility curve in the earthquake-only scenario at the performance level of LS. But, the probability of collapse increases in the PEF scenario at higher maximum accelerations. Therefore, the general shape of the fragility curve of the structure in the PEF scenario can be considered to be approximately the same as the fragility curve shape in the earthquake scenario at the LS performance level.
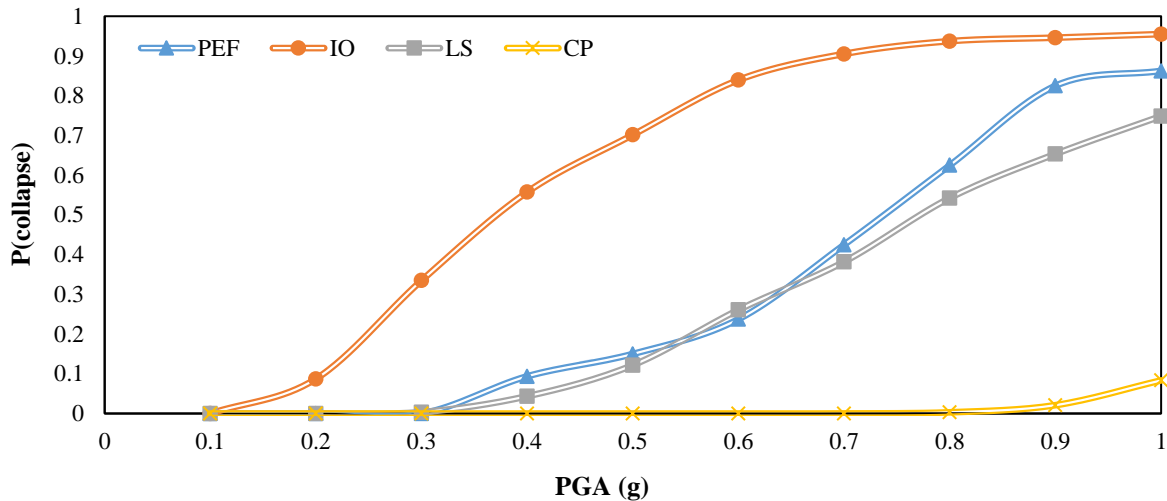
Fig. 20. Fragility curve of the intended frame subjected to the definite events of earthquake and PEF scenarios

4. Conclusions

In the present study, the behavior of a 4-story reinforced concrete frame was surveyed during the PEF scenario based on the probabilistic foundations. The collapse time of the frame during a PEF loading was the most significant parameter of this research. A 4-story reinforced concrete frame has been analyzed based on IDA. Ten grand motions were applied to this frame from 0.1g to 1g. After each seismic load, the thermal load was applied to the frame. For thermal loading, four different fire loads were considered in four different locations and situations of the frame. The results of the analysis showed 70% of loading the structures were able to withstand a durability time equal to or longer than 120 minutes. In 15% of the scenarios, the collapse time in a PEF was shorter than 1 hour. Then the PDF and CDF curve was extracted for a definite event of the post-earthquake scenario. The results showed that PGA and situation of fire loading affected frame resistance under PEF loading. Also, the results of the analysis showed that the fragility curve in the PEF scenario based on the maximum applied acceleration to the structure was very similar to the fragility curve in the earthquake scenario at the LS performance level. The probability of an annual collapse of the structure in the PEF scenario was investigated. For the considered frame, the

annual rate was equal to 0.00036.

The results of this study can be used to assess the probability of rupture of reinforced concrete frames in post-earthquake fire scenario. With seismic fragility curves at the LS level, it is possible to estimate the probability of a break in the loading of a post-earthquake fire at different seismic load intensities. These results can be used to calculate the probability of annual failure due to post-earthquake fire.

5. Acknowledgments

6. References

Abdollahzadeh, G. and Faghihmaleki, H. (2018). "Proposal of a probabilistic assessment of structural collapse concomitantly subject to earthquake and gas explosion", *Frontiers of Structural and Civil Engineering,* 12(3), 425-437.

Albuquerque, G.L., Silva, A.B., Rodrigues, J.P.C. and Silva, V.P. (2018). "Behavior of thermally restrained RC beams in case of fire", *Engineering Structures,* 174, 407-417.

Behnam, B., Ronagh, H.R. and Lim, P.J. (2016). "Numerical evaluation of the post-earthquake fire resistance of CFRP-strengthened reinforced concrete joints based on experimental observations", *European Journal of Environmental and Civil Engineering,* 20(2), 142-160.

Behnama, B. and Ronagh, H.R. (2013). "Post-earthquake fire performance-based behavior of reinforced concrete structures", *Earthquakes and Structures,* 5(4), 379-394.

BSSC, P. (2000). *Commentary for the seismic rehabilitation of building*, FEMA-356, Federal Emergency Management Agency, Washington, DC.

Chicchi, R. and Varma, A.H. (2018). "Research review: Post-earthquake fire assessment of steel buildings in the United States", *Advances in Structural Engineering,* 21(1), 138-154.

Elhami Khorasani, N. (2015). *A probabilistic framework for multi-hazard evaluations of buildings and communities subject to fire and earthquake scenarios,* Ph.D. Thesis, Princeton University, USA.

Elhami Khorasani, N. and Garlock, M.E. (2017). "Overview of fire following earthquake: Historical events and community responses", *International Journal of Disaster Resilience in the Built Environment,* 8(02), 158-174.

Hutchinson, T., Wang, X., Hegemier, G., Meacham, B. and Kamath, P. (2018). "Physical damage evolution during earthquake and post-earthquake fire testing of a mid-rise cold-formed steel framed building", *Proceedings of the 11th US National Conference on Earthquake Engineering*, Loss Angeles.

Imani, R., Mosqueda, G. and Bruneau, M. (2014). "Experimental study on post-earthquake fire resistance of ductile concrete-filled double-skin tube columns", *Journal of Structural Engineering,* 141(8), 04014192.

Jelinek, T., Zania, V. and Giuliani, L. (2017). "Post-earthquake fire resistance of steel buildings", *Journal of Constructional Steel Research,* 138, 774-782.

Khorasani, N.E., Garlock, M. and Gardoni, P. (2016). "Probabilistic performance-based evaluation of a tall steel moment resisting frame under post-earthquake fires", *Journal of Structural Fire Engineering,* 54(3), 361-374.

Khorasani, N.E., Gernay, T. and Garlock, M. (2017). "Data-driven probabilistic post-earthquake fire ignition model for a community", *Fire Safety Journal,* 94, 33-44.

Mohammadizadeh, M.R., and Jafarzadeh, A. (2021). "Comparison of nonlinear dynamic analysis of time history and Endurance Time Method in tall structures with fame-wall system", *Civil Engineering Infrastructures Journal* 54(2), 405-421.

Moradi, M. and Abdolmohammadi, M. (2020). "Seismic fragility evaluation of a diagrid structure based on energy method", *Journal of Constructional Steel Research,* 174, 106311.

Moradi, M., Tavakoli, H. and Abdollahzade, G. (2020). "Sensitivity analysis of the failure time of reinforcement concrete frame under postearthquake fire loading", *Structural Concrete,* 21(2), 625-641.

Moradi, M., Tavakoli, H. and Abdollahzadeh, G. (2019). "Probabilistic assessment of failure time in steel frame subjected to fire load under progressive collapses scenario", *Engineering Failure Analysis,* 102, 136-147.

Moradi, M., Tavakoli, H.R. and Abdollahzadeh, G.R. (2021). "Comparison of steel and reinforced concrete frames' durability under fire and post-earthquake fire scenario", *Civil Engineering Infrastructures Journal,* 54(1), 145-168.

Ronagh, H.R. and Behnam, B. (2012). "Investigating the effect of prior damage on the post-earthquake fire resistance of reinforced concrete portal frames", *International Journal of Concrete Structures and Materials,* 6(4), 209-220.

Tang, Z., Zhang, W., Yu, J. and Pospíšil, S. (2020). "Post-earthquake strength assessment of a steel bridge considering material strength degradation", *Structure and Infrastructure Engineering*, 17(3), 331-346.

Tavakoli, H. and Afrapoli, M.M. (2018). "Robustness analysis of steel structures with various lateral load resisting systems under the seismic progressive collapse", *Engineering Failure Analysis,* 83, 88-101.

Tavakoli, H. and Kiakojouri, F. (2015). "Threat-independent column removal and fire-induced progressive collapse: Numerical study and comparison", *Civil Engineering Infrastructures Journal,* 48(1), 121-131.

Vitorino, H., Rodrigues, H. and Couto, C. (2020). "Evaluation of post-earthquake fire capacity of reinforced concrete elements", *Soil Dynamics and Earthquake Engineering,* 128, 105900.

Wen, B., Wu, B. and Niu, D. (2016). "Post-earthquake fire performance of reinforced concrete columns", *Structure and Infrastructure Engineering,* 12(9), 1106-1126.